THE JOURNAL OF PHYSICAL CHEMISTRY B

Article

pubs.acs.org/JPCB

Designing J- and H-Aggregates through Wave Function Overlap Engineering: Applications to Poly(3-hexylthiophene)

Hajime Yamagata, Chris M. Pochas, and Frank C. Spano*

Department of Chemistry, Temple University, Philadelphia, Pennsylvania 19122, United States

Supporting Information

ABSTRACT: A novel mechanism for J- and H-aggregate formation is presented on the basis of wave function overlap (WFO) coupling between neighboring chromophores which supplements the usual through-space (Coulombic) coupling. In cases where the latter is relatively small compared to the former, as might arise for excitons based on molecular transitions with low oscillator strengths, J- vs H-aggregation is determined by the sign of the product D_eD_h, where D_e (D_h) is the coupling between a neutral Frenkel exciton and the charge transfer exciton created through the transfer of an electron (hole) to a neighboring chromophore. Adapting a sign convention based on translational symmetry in a linear array of chromophores, a positive (negative) sign for D_eD_h places the bright exciton on the bottom (top) of the exciton band, consistent with J- (H-) aggregation. The J- (H-) aggregates so formed behave as direct (indirect) bandgap semiconductors with vibronic signatures in absorption and photoluminescence that are identical to those displayed by conventional Coulomb coupled aggregates. WFO coupling leading to the mixing of intrachain Frenkel excitons and polaron pairs may be important in conjugated polymer aggregates where the Coulomb coupling practically vanishes with the (conjugation) length of the polymer. Calculations based on octathiophene (8T) dimers show that the eclipsed geometry yields a WFO coupling favoring H-aggregate behavior, although a longitudinal (long-axis) displacement by only 1.5 Å is enough to change the sign of the coupling, leading to J-aggregate behavior. Hence, it should be possible to design thiophene-based polymers which act as J-aggregates with respect to the interchain coupling.

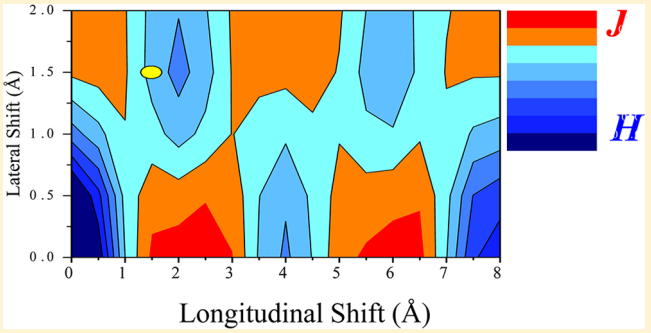

I. INTRODUCTION

The conventional view of molecular H- and J-aggregates considers the origin of the intermolecular coupling to be Coulombic; for example, dipole−dipole coupling between a given pair of chromophores is often assumed.[1] The sign of the coupling, as determined by the relative orientation of the chromophores, causes a blue (red) shift of the main absorption peak in H- (J-) aggregates and an attenuation (amplification) of the radiative decay rate. Recently, vibronic signatures differentiating H- and J-aggregation have been discovered on the basis of how the coupling impacts the redistribution of oscillator strength away from the Poisonnian distribution characteristic of unaggregated monomers.[2] In conjugated molecules, the main progression forming mode is related to the CC symmetric stretching mode (or modes) occurring around 1400 cm^{-1}. Vibronic signatures are often superior in identifying J- or H-aggregation as spectral shifts may have several causes, for example, the omnipresent nonresonant gas-to-crystal red-shift. The latter can be large enough to obscure the excitonic blue shift in weakly coupled H-aggregates, leading to an incorrect assignment.[3]

Through-space (Coulombic) coupling leads to a direct transfer of excitation between chromophores operative over long distances ($\lesssim$ 10 nm), as described by Forster theory and its many extensions.[4−12] When the coupling is coherent, as is often the case between nearby and resonant chromophores, conventional J- and H-aggregates are formed, dictated by the sign of the Coulombic coupling. In many molecular aggregates, neighboring molecules are close enough so that their wave functions overlap, allowing also for charge transfer. The coupling between adjacent HOMOs (LUMOs) on neighboring molecules is dictated by the charge resonance integral t_{HOMO} (t_{LUMO}). Such interactions lead to the formation of conduction and valence bands and necessitate the inclusion of charge-transfer (CT) configurations in excited electronic states; for example, CT allows the molecular excited state, S_1, to couple to the CT state created when an electron in the LUMO of the excited molecule is transferred to the LUMO of an unexcited neighbor. (Conversely, an electron in the HOMO of an unexcited neighboring molecule may move to the HOMO of the excited molecule, a process normally referred to as hole transfer). The resulting CT excitons play a prominent role in the optical properties of molecular crystals.[13−17]

Received: September 21, 2012
Revised: November 15, 2012

   dx.doi.org/10.1021/jp309407r | J. Phys. Chem. B XXXX, XXX, XXX−XXX

In what follows, we show that the short-range coupling between Frenkel and CT excitons, as mediated by t_{HOMO} and t_{LUMO}, can create H- and J-aggregates which conform with all of the vibronic spectral signatures associated with conventional aggregates. In other words, *H- and J-aggregates can exist in the absence of Coulombic coupling*. The mechanism is easiest to appreciate using perturbation theory; we assume, as is often true of molecular crystals, that the magnitudes of t_{HOMO} and t_{LUMO} are smaller than the energy gap between the higher-energy CT exciton and the (localized) molecular excitation, $E_{CT} - E_{S_1}$. Neglecting for the moment through-space Coulombic coupling, the energetic shifts induced by the Frenkel/CT interactions result in a level ordering of the delocalized eigenstates characteristic of J- or H-aggregates (with the bright state respectively residing at the bottom or top of the exciton band) depending on the *relative* signs of t_{HOMO} and t_{LUMO}. This is best appreciated from the form of the effective coupling between two chromophores, $2t_{HOMO}t_{LUMO}/(E_{CT} - E_{S_1})$, obtained using second-order perturbation theory. Here, an electronic excitation is effectively transferred to a neighboring molecule through a two-step process in which an electron transfer is followed by a hole transfer (and vice versa). The higher-energy CT intermediate state is only *virtually* excited. A more rigorous treatment of this type of coupling has been given by Harcourt et al.[18,19] The coupling mechanism is similar to Dexter exchange in that it depends critically on wave function overlap (WFO).[20] We therefore refer to the CT mediated coupling described above as WFO coupling. It is operative in both singlet and triplet exciton transfer. When WFO coupling exceeds through-space Coulombic coupling, the nature of the aggregate—J or H—is entirely determined by the sign of $t_{HOMO}t_{LUMO}$.

The current work is particularly relevant for aggregates of conjugated polymers, where the CT state, more commonly referred to as a polaron pair, plays an important role in determining polymer film photophysics.[21,22] In spin-cast poly(3-hexylthiophene) (P3HT) films, interchain (Coulombic) coupling leads to H-aggregate signatures in absorption and emission. However, as shown by several groups, the interchain coupling practically vanishes as the polymer chain length increases.[9,23−26] By contrast, calculations by Gierschner et al.[26] show that t_{HOMO} and t_{LUMO} are relatively stable with chain length. Hence, the WFO coupling leading to Frenkel/polaron pair mixing[27,28] may dominate in the limit of exceptionally well-ordered polymer assemblies, where long conjugation lengths preclude strong Coulombic coupling. However, in typical spin-cast P3HT films prepared to date, the presence of substantial intrachain disorder limits the effective chain (conjugation) length, most likely leading to dominant Coulombic interactions. Better processing conditions, such as those leading to the creation of well-ordered P3HT nanofibers,[29] favor WFO coupling.

As has been shown previously for a variety of chromophores, the magnitudes and signs of t_{HOMO} and t_{LUMO} are particularly sensitive to the intermolecular orientations, having important implications for charge transport.[30−33] A very recent study by Beljonne and co-workers on donor−acceptor copolymers underscored the sensitivity of transport properties to a relative displacement (slide) of neighboring polymers along the long-molecular axis.[33] Since t_{HOMO} and t_{LUMO} also impact optical properties through WFO coupling, the latter also sensitively depends on the relative shift between neighboring chains, both along and normal to the long-molecular axis. The sensitivity of WFO coupling to intermolecular orientations may play a role in the recent observations of J-like behavior in P3HT nanofibers reported by several groups,[29,34] although one must also consider the intrinsic J-like influence of *intra*chain coupling.[35]

In what follows, we will investigate the photophysical properties of a cofacial dimer complex consisting of two thiophene oligomers, each consisting of eight thiophene rings. We begin by determining how t_{HOMO} and t_{LUMO}, as calculated using quantum chemical methods, are affected by sliding one chain relative to the other while maintaining a fixed interchain distance of 3.8 Å, the interchain contact distance in P3HT.[36,37] The ensuing analysis of the photophysical properties is based on an exciton Hamiltonian which includes charge transfer excitations as well as vibronic coupling to the main thiophene ring symmetric stretching mode in the vicinity of 1400 cm^{-1}. We evaluate absorption and temperature-dependent photoluminescence (PL) spectra to demonstrate that WFO coupled H- and J-aggregates display the same vibronic spectral signatures as their Coulombically coupled counterparts. When perturbation theory is applicable, the Hamiltonian reduces to an effective Frenkel Hamiltonian, from which the WFO coupling can be readily identified. We discuss the prospect of creating interchain J-aggregates of thiophene-based polymers by controlling the relative orientation of neighboring chains.

II. ORIENTATION-DEPENDENT TRANSFER INTEGRALS

We begin with an analysis of WFO coupling in a dimer consisting of the octathiophene (8T) oligomers shown in Figure 1, focusing first on how the interchain LUMO and

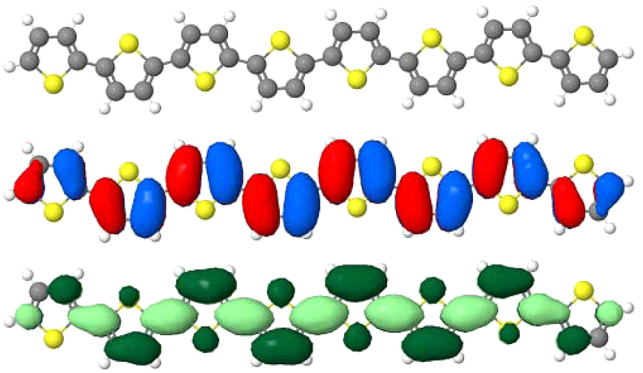

Figure 1. The molecular structure of 8T along with its HOMO (upper) and LUMO (lower).

HOMO splittings, governed by t_{LUMO} and t_{HOMO}, respectively, depend on the relative orientation of the two molecules. We assume that the long axes of the two oligomers remain parallel and vary the longitudinal (along the long-axis) and lateral (along the short-axis) displacements, anticipating applications to poly(3-hexylthiophene) π-stacks. As we will show in the following section, the sign of the effective excitonic coupling between two oligomers depends on the sign of the product $t_{HOMO} \times t_{LUMO}$. Hence, the *relative* sign between t_{HOMO} and t_{LUMO} ultimately determines H- or J-aggregate behavior.

We first optimized the geometry of a single 8T molecule at the HF/6-31G(d) level. We chose 8T, since it is large enough to minimize end effects and therefore mimic the polymer but small enough to be efficiently handled within our computational resources. In the geometry minimization, the C_{2h}

dx.doi.org/10.1021/jp309407r | J. Phys. Chem. B XXXX, XXX, XXX−XXX

symmetry was maintained so that the molecule remains planar. The geometry of the second molecule is a duplicate of the first. Both molecules are taken to be cofacially oriented and placed 3.8 Å apart. Orbital energies of the dimer assembly are evaluated at the ZINDO level. In the analysis, the magnitude of t_{HOMO} (t_{LUMO}) is taken to be half of the HOMO (LUMO) splitting upon dimerization. This is rigorous as long as there exists a symmetry operation which interchanges the two molecules. The absence of symmetry invites the possibility of different molecular excitation energies, making the dimer splitting a function of the transfer integrals *and* the excitation energy difference.[31]

In the staggered dimer shown in Figure 2a, both molecules are related by a $\hat{C}_2$ rotation. C_2 point group symmetry is

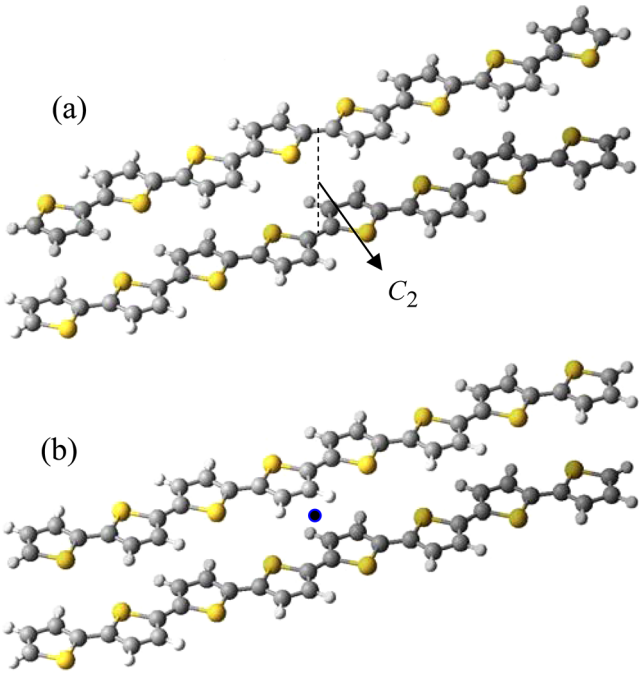

Figure 2. Staggered (a) and eclipsed (b) dimers of 8T.

maintained as the two molecules slip relative to each other along a direction parallel to the long molecular axes. In the eclipsed dimer of Figure 2b, the two molecules are related though an inversion operation, with the center indicated by the blue dot. In this case, C_i point group symmetry is maintained as the molecules undergo a longitudinal displacement.

The dimer MOs for the staggered dimer of Figure 2a are shown in Figure 3. They are either symmetric (S) or antisymmetric (AS) with respect to the C_2 rotation. The phases of the MOs localized on molecules A and B, labeled h_A, l_A, h_B, and l_B in the figure, are chosen such that

$$l_B = \hat{C}_2 l_A \tag{1a}$$

and

$$h_B = \hat{C}_2 h_A \tag{1b}$$

With this phase convention, the in-phase combination of the two localized LUMOs, $L_1 = l_A + l_B$, is symmetric under the $\hat{C}_2$ rotation, while the out-of-phase combination, $L_2 = l_A - l_B$, is antisymmetric. Since the energy of the in-phase orbital L_1 is lower than the out-of-phase orbital L_2 (see Figure 3), the sign of the coupling, t_{LUMO}, must be negative. Continuing, we find

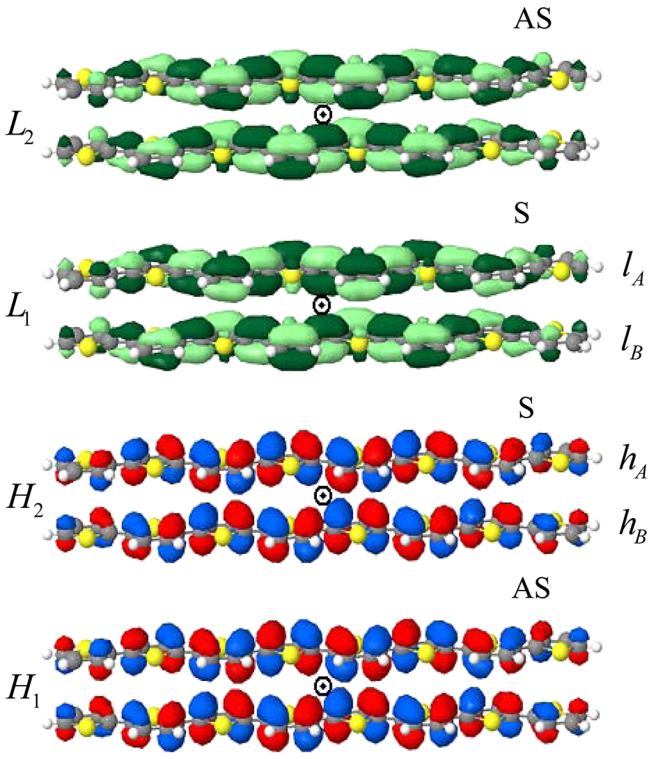

Figure 3. Four frontier molecular orbits corresponding to the staggered 8T dimers of Figure 2a with the C_2 axis normal to the page as indicated. H_2 and L_1 are the HOMO and LUMO, respectively. Orbital symmetries (S, AS) with respect to the C_2 rotation are indicated on the upper right of each MO. For the eclipsed dimer (not shown), the MO symmetries defined with respect to an inversion operation follow the same pattern with increasing energy (AS, S, S, AS).

the ordering is reversed in the occupied MO's: $H_1 = h_A - h_B$ and $H_2 = h_A + h_B$ are respectively antisymmetric and symmetric. Since the in-phase orbital is now higher in energy, t_{HOMO} must be positive.

Figure 4a shows t_{HOMO} and t_{LUMO} as a function of the longitudinal displacement d for the C_2 dimer, starting in the staggered geometry ($d = 0$) shown in Figure 2a. The signs were determined from the energetic ordering of the in- and out-of-phase states using the C_2 phase convention in eq 1. Both t_{HOMO} and t_{LUMO} show oscillations similar to those observed by Bredas et al.[30] for 6T dimers. (In ref 30, the splitting *magnitudes* are plotted vs *d*.) Figure 4a shows that both couplings display an oscillation period of approximately 8 Å, the length of two thiophene units. The slight deviation from exact periodicity is due to end-effects. Further observation reveals a "quasi" period of 4 Å, indicating that the coupling is dominated by ring overlap (whether staggered or eclipsed). Coupling is slightly larger in the eclipsed configuration due to more efficient inter-ring overlap. Figure 4a further shows that t_{HOMO} varies more strongly than t_{LUMO}. This can be accounted for by referring to the MOs in Figure 1. The lobes of the single chain LUMO are oriented along the chain, in contrast to the cross-chain orientation of the HOMO lobes, making t_{HOMO} more easily influenced by the longitudinal shift than t_{LUMO}. In addition, t_{LUMO} remains uniformly negative while the sign of t_{HOMO} alternates with the shift. Therefore, the sign of the *product* t_{HOMO} t_{LUMO} also alternates. As we will see below, the sign of the product determines J- or H-aggregate behavior.

dx.doi.org/10.1021/jp309407r | J. Phys. Chem. B XXXX, XXX, XXX–XXX

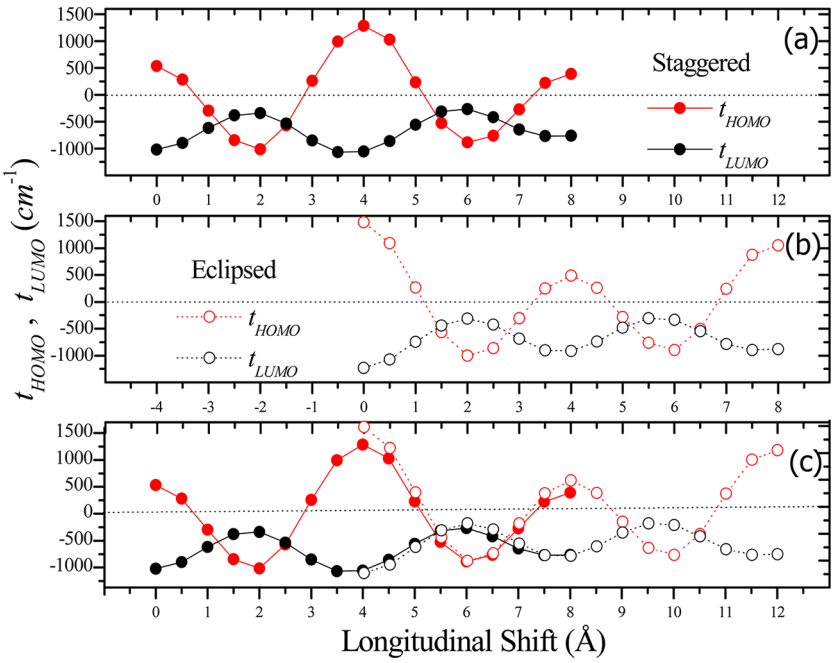

Figure 4. t_{LUMO} and t_{HOMO} vs the longitudinal shift d. In part a, d = 0 corresponds to the staggered geometry in Figure 2a, while, in part b, d = 0 corresponds to the eclipsed geometry in Figure 2b. The two are combined in part c, where d = 0 corresponds to the staggered form.

In Figure 4b, the analysis is repeated for the C_i dimer, starting with the eclipsed geometry when d = 0 (see Figure 2b). Since inversion symmetry is maintained during the slide, the phase convention is established by replacing the $\hat{C}_2$ operation by the inversion operation, $\hat{i}$, in eqs 1a and 1b. Figure 4b shows that the eclipsed configuration corresponds closely with the point d = 4 Å in the C_2 dimer of Figure 4a. This is so because, in the latter configuration, seven of the eight rings are eclipsed with a remaining "unpaired" ring on either side. The magnitudes of our calculated couplings agree well with those calculated for OT6 dimers in ref 30 (our couplings are slightly larger since we use an intermolecular separation of 3.8 Å vs 4 Å in ref 30). The two curves from Figure 4a and b are drawn together in part c. The curves do not overlap completely due to the aforementioned end effects, which are expected to vanish entirely as the oligomer length increases.

In addition to the longitudinal shift, we also investigated lateral shifts along the short molecular axis. Figure 5 shows how t_{HOMO} and t_{LUMO} vary with the longitudinal displacement for several lateral displacements in the C_i dimer. The figure shows that t_{LUMO} is far more sensitive to lateral shifting than t_{HOMO}. This once again is attributed to the nodal distribution in the LUMO vs the HOMO of the single chain (Figure 3). Figure 5 shows that for a sufficiently large lateral shift t_{LUMO} becomes positive.

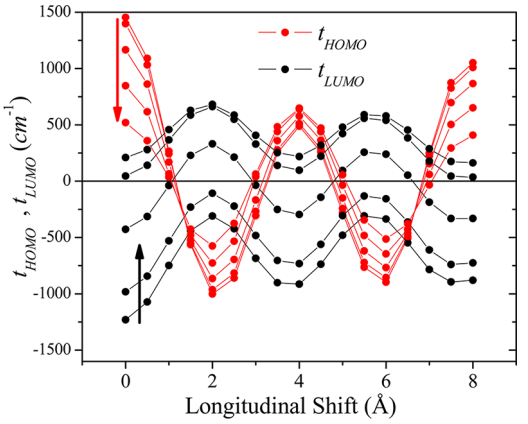

Figure 5. t_{LUMO} and t_{HOMO} vs the longitudinal shift for several values of lateral displacement in the C_i dimer. Values of the lateral displacement are taken in steps of 0.5 Å, starting at 0. Arrows indicate the direction of increasing lateral shift.

III. WFO COUPLED J- AND H-DIMERS

Let us now consider the optical properties of the C_2 dimers of Figure 2a. The analysis is identical for the eclipsed dimers of Figure 2b after replacing $\hat{C}_2$ with $\hat{i}$ in what follows. It is essential that the sign convention assumed in assigning the phases of t_{HOMO} and t_{LUMO} be maintained in choosing the phases of the optical excitations comprising the Frenkel excitons. The latter are constructed from molecular excitations S_1 which are largely comprised of the HOMO−LUMO excitations within a single oligomer ($h_A \rightarrow l_A$). As such, the $S_0 \rightarrow S_1$ transition dipole is directed mainly along the long molecular axis. Since the ground electronic state (both molecules in the state S_0) is symmetric and the transition dipole moment vector is antisymmetric under $\hat{C}_2$, then only the antisymmetric Frenkel exciton

$$|F_{AS}\rangle = 2^{-1/2}\{|A\rangle - |B\rangle\} \quad (2)$$

can be optically excited from the ground electronic state. Here $|A\rangle$ ($|B\rangle$) indicates oligomer A (B) is in the electronic excited state, S_1, with the remaining oligomer unexcited in S_0. The relative phases of $|A\rangle$ and $|B\rangle$ are established in exactly the same way as the relative phases of the molecular orbitals; i.e., for the C_2 dimer, $|B\rangle = \hat{C}_2|A\rangle$, which is consistent with $h_B l_B = \hat{C}_2 h_A l_A$. With this phase convention, the transition dipole moment to the bright exciton in eq 2 is given by

$$\langle G|\hat{\mu}|F_{AS}\rangle = \frac{1}{\sqrt{2}}(\boldsymbol{\mu}_A - \boldsymbol{\mu}_B) = \sqrt{2}\boldsymbol{\mu}_A \quad (3)$$

dx.doi.org/10.1021/jp309407r | J. Phys. Chem. B XXXX, XXX, XXX−XXX

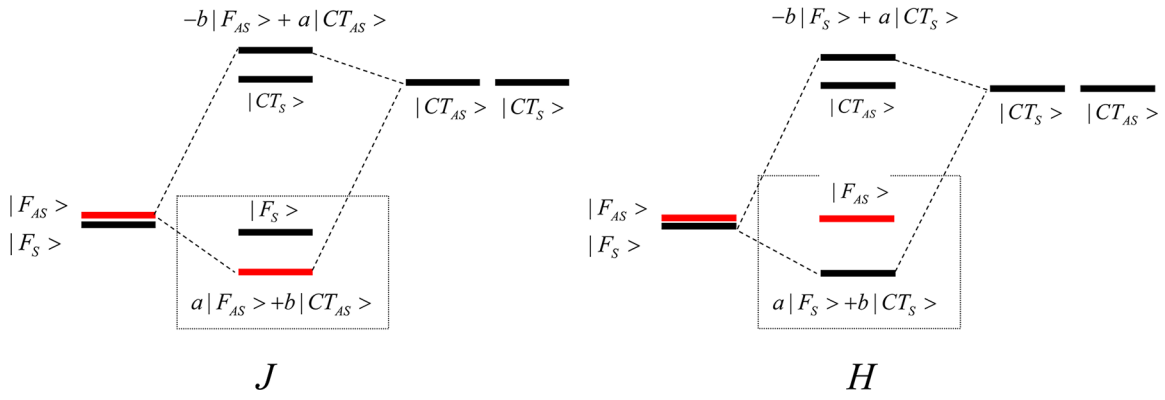

Figure 6. Energy level diagrams demonstrating the formation of WFO coupled J- and H-aggregates. Red levels correspond to bright states. State symmetries are based on a C_2 rotation (see text). In the scheme on the left, $D_e = -D_h$ is taken so that only the antisymmetric (bright) Frenkel and CT excitons mix. The bright exciton is therefore repelled to the bottom of the band, making a J-aggregate. The scheme on the right side corresponds to $D_e = D_h$. Now, only the symmetric states mix, repelling the dark state to the band bottom as in an H-aggregate. See text for additional details.

where $\hat{\mu}$ is the dipole moment operator and $|G\rangle$ is the dimer ground state. $\boldsymbol{\mu}_A$ and $\boldsymbol{\mu}_B$ are the molecular transition dipole moments for molecules A and B, respectively. Because $\boldsymbol{\mu}_B = \hat{C}_2\boldsymbol{\mu}_A$, the two transition dipoles oppose each other, $\boldsymbol{\mu}_B = -\boldsymbol{\mu}_A$. Conversely, the symmetric Frenkel exciton

$$|F_S\rangle = 2^{-1/2}\{|A\rangle + |B\rangle\} \tag{4}$$

is dark, since its transition dipole moment is exactly zero.

Frenkel excitons like those in eqs 2 and 4 can only couple to CT states with the same symmetry. The symmetric and antisymmetric CT states are, respectively, given by

$$|CT_S\rangle = 2^{-1/2}\{|A^+B^-\rangle + |A^-B^+\rangle\} \tag{5a}$$

$$|CT_{AS}\rangle = 2^{-1/2}\{|A^+B^-\rangle - |A^-B^+\rangle\} \tag{5b}$$

Here, $|A^-B^+\rangle$ ($|A^+B^-\rangle$) consists of an electron (hole) on A and a hole (electron) on B. The phase relation, $|A^-B^+\rangle = \hat{C}_2|A^+B^-\rangle$, is consistent with the MO phase convention in eq 1.

CT and Frenkel excitons of the same symmetry will couple when there is sufficient overlap between HOMO and LUMO wave functions on neighboring molecules. The WFO coupling between the two symmetric states (eqs 4 and 5a) is given by the quantity $D_e + D_h$, while the coupling between the two antisymmetric states (eqs 2 and 5b) is given by $D_e - D_h$. Here, D_e (D_h) is the electron (hole) dissociation integral connecting a molecular excitation on a given molecule with the CT state created by transfer of an electron (hole) to a neighboring molecule. To a good approximation, the dissociation integrals are related to the HOMO and LUMO transfer integrals as

$$D_e \equiv \langle A|\hat{H}|A^+B^-\rangle \approx t_{LUMO} \tag{6a}$$

$$D_h \equiv \langle A|\hat{H}|A^-B^+\rangle \approx -t_{HOMO} \tag{6b}$$

On the basis of the discussion above, we can readily appreciate how Frenkel/CT mixing can induce J- or H-aggregate behavior in cases where the through-space Coulombic coupling is negligible. In all that follows, we take the energy of the CT states, E_{CT}, to be higher than the molecular transition energy E_{S_1}, as is the case in many polyacene molecular crystals where the CT state is at least several hundred meV's higher than the parent Frenkel states.[13,14] The mixing between the antisymmetric bright Frenkel exciton in eq 2 and the higher energy antisymmetric CT state in eq 5b causes the energy of the former to be repelled downward by an amount governed by the difference $|D_e - D_h|$. Mixing between the (symmetric) optically dark exciton and the symmetric CT exciton also causes a downward energy shift but with a magnitude governed by the sum, $|D_e + D_h|$. Hence, we find that, as in an H-aggregate, the bright exciton is higher in energy than the dark exciton whenever

$$D_eD_h > 0 \qquad \text{H-like } (C_2 \text{ and } i \text{ Phase Convention}) \tag{7a}$$

Conversely, the bright exciton is the lowest energy exciton, as in a J-aggregate, whenever

$$D_eD_h < 0 \qquad \text{J-like } (C_2 \text{ and } i \text{ Phase Convention}) \tag{7b}$$

When the CT energy is large enough to satisfy the condition

$$E_{CT} - E_{S_1} \gg |D_e|, |D_h| \tag{8}$$

we can use second-order perturbation theory to determine the energy of the mixed states. Under this condition, the energies of the bright and dark excitons are given by

$$E_{AS} = E_{S_1} - \frac{(D_e - D_h)^2}{E_{CT} - E_{S_1}}, \qquad \text{bright exciton} \tag{9a}$$

and

$$E_S = E_{S_1} - \frac{(D_e + D_h)^2}{E_{CT} - E_{S_1}}, \qquad \text{dark exciton} \tag{9b}$$

The J/H-aggregate formation mechanism is demonstrated schematically in Figure 6 for two extreme cases: $D_e = -D_h$ and $D_e = D_h$. In the former case, only the antisymmetric (bright) states mix, causing the antisymmetric state to be pushed below the symmetric state, resulting in a WFO coupled J-aggregate. Moreover, since the wave function coefficients satisfy $|a| \gg |b|$ and CT states carry negligible oscillator strengths, the two highest energy excitons carry very little oscillator strength. Hence, photophysical properties are mainly determined by the lowest energy excitons contained in the box of Figure 6. When $D_e = D_h$, the situation is reversed; now, only the (dark) symmetric states mix, resulting in a dark lowest energy state, as is characteristic of H-aggregates. This is depicted in the right-hand side of Figure 6. Note that weak, through-space Coulombic coupling, $J_{TS} \ll E_{CT} - E_{S_1}$, can easily be

dx.doi.org/10.1021/jp309407r | J. Phys. Chem. B XXXX, XXX, XXX−XXX

incorporated in Figure 6 by adding J_{TS} ($-J_{TS}$) to the final energy of the mixed symmetric (antisymmetric) exciton.

From Figure 4a and eq 6, we have $D_eD_h > 0$ for the staggered dimer of Figure 2a. It should therefore behave as an H-aggregate with respect to WFO coupling. Further reference to Figure 3 shows that the HOMO−LUMO transition is not allowed, since both orbitals are symmetric and the dipole moment operator is antisymmetric with respect to $\hat{C}_2$. Hence, WFO coupled H-aggregates are indirect bandgap semiconductors. Conversely, WFO coupled J-aggregates are direct bandgap semiconductors.

Aggregates with Translational Symmetry. We emphasize that making H/J assignments based on the inequalities in eqs 7a and 7b assumes the C_2 or i phase conventions, as are appropriate for the dimers of Figure 2a and 2b, respectively. In linear aggregates comprised of two or more chromophores (with periodic boundary conditions), the phases of the MOs and optically excited states are, by the usual convention, based on operations which translate molecules by the unit vectors along the chain, i.e., $l_B = \hat{T}l_A$ and $h_B = \hat{T}h_A$ in place of eqs 1a and 1b. In this case, the 8T transition dipole moment is now *symmetric* under the operation ($\hat{T}$) defining the phase convention. The bright state is the totally symmetric ($k = 0$) exciton which couples to the $k = 0$ CT states with the value $D_e + D_h$. Hence, when D_e and D_h have the *same* sign, one creates a J-aggregate, while an H-aggregate requires D_e and D_h to have opposite signs, in contrast to what is found on the basis of the C_2 (or i) phase convention in eqs 7a and 7b. We therefore have under translational symmetry

$$D_eD_h > 0 \qquad \text{J-like (T Phase Convention)} \tag{10a}$$

$$D_eD_h < 0 \qquad \text{H-like (T Phase Convention)} \tag{10b}$$

The translation convention was adapted in our analysis of a single polymer chain in ref 38. Most importantly, although the signs of D_e and D_h depend on the chosen phase convention, the physical properties—including the J or H assignment—do not. This is readily appreciated by considering the eclipsed dimer in Figure 2b which has an inversion center as well as translational symmetry. Under the i convention, Figure 4b and eq 6 give $D_eD_h > 0$, but under the T convention, $D_eD_h < 0$. Both cases represent an H-aggregate/indirect bandgap semiconductor.

In this section, we have shown that WFO coupling can induce the energy level ordering corresponding to J- or H-aggregates. In the following section, we test to see if the vibronic signatures of J- and H-aggregation worked out previously for Coulombic coupling[2] remain valid for the WFO coupled aggregates.

IV. VIBRONIC SIGNATURES IN ABSORPTION AND EMISSION

The Hamiltonian for the WFO coupled aggregates takes the form of an exciton Hamiltonian including charge transfer between neighboring molecules[39] as well as vibronic coupling to the main, progression forming mode, as treated by Holstein.[40] The Hamiltonian is essentially identical to that used earlier to describe absorption in tetracene crystals.[16] As the complete Hamiltonian is quite cumbersome, we relegate it to the Supporting Information. The Hamiltonian also strongly resembles the Wannier exciton Hamiltonian used in ref 38 to describe the photophysics of a single polymer chain, where the thiophene units were considered to be head-to-tail coupled chromophores. In this section, we utilize the Hamiltonian in eq S1 (Supporting Information) to investigate absorption and emission in the J-like and H-like WFO coupled dimers introduced in the last section. Details of the spectral calculations are also included in the Supporting Information.

We begin by checking whether the sign of the product D_eD_h determines J- or H-aggregation with respect to the vibronic signatures outlined in ref 2. Briefly, they are as follows: (1) In an H-aggregate (J-aggregate), the ratio of the intensities of the first two peaks (A_1 and A_2) in the vibronic progression of the absorption spectrum is attenuated (enhanced) relative to the monomer ratio, $1/\lambda^2$, where λ^2 is the Huang−Rhys factor. (2) In an H-aggregate without disorder and at $T = 0$ K, there is no 0−0 peak in the PL spectrum. Increasing temperature increases 0−0 emission due to thermal activation of the $k = 0$ exciton at the top of the lowest energy vibronic band. In a J-aggregate, 0−0 emission is enhanced (superradiant) when there is no disorder and diminishes with increasing temperature due to depletion of the $k = 0$ exciton population. There is also ideally no Stokes shift, since the same state is responsible for the absorption origin (A_1) and emission origin (0−0).

Figure 7 shows absorption and PL spectra for two WFO coupled dimers each with C_2 symmetry. Two limiting cases are shown: $D_e = D_h = 0.1$ eV and $D_e = -D_h = -0.1$ eV. We further took $E_{CT} - E_{S_1} = 1.0$ eV and a vibrational energy of $\hbar\omega_0 = 0.17$ eV (1400 cm^{-1}). The HR factor regulating the exciton−vibrational coupling was set to unity ($\lambda^2 = 1$) so that the A_1 and A_2 peaks in the absorption spectrum of a monomer are of equal intensity, as is also true of the 0−0 and 0−1 peaks in the reduced PL spectrum. (Here, we define the reduced PL spectrum to be the PL spectrum without the cubic frequency dependence; see the Supporting Information.) Figure 7 clearly shows the changeover from H- to J-aggregate behavior based on the aforementioned spectral signatures when the sign of D_eD_h changes from positive to negative, consistent with the C_2 phase convention of eq 7. As an additional test, we took one of the transfer integrals to be zero, for example, $D_e = 0$ and $D_h = 0.1$ eV (not shown). We obtained essentially the *same spectral intensity distributions as in the monomer*; i.e., the A_1 and A_2 peaks in the absorption spectrum are of equal intensity, the 0−0 and 0−1 peaks in the reduced PL spectrum are of equal intensity, and the PL spectrum is temperature independent. Hence, when either D_e or D_h are zero, the dimer behaves as if there is no coupling between chromophores. There is, however, a spectral red-shift due to the remaining nonzero dissociation integral.

Effective Hamiltonian. Conventional wisdom suggests that in order to intraconvert J- and H-aggregate behavior one must change the sign of the coupling between chromophores. Figure 7 demonstrates that such a coupling should depend on the product D_eD_h. In order to develop a more quantitative understanding of this relationship, we introduce the effective Frenkel exciton Hamiltonian.

When the condition in eq 8 is maintained along with the additional requirements that the vibrational energy and through-space Coulombic coupling remain significantly smaller than the CT/S_1 gap, i.e., when

$$|D_e|, |D_h|, |J_{TS}|, \hbar\omega_0 \ll E_{CT} - E_{S_1} \tag{11}$$

is satisfied, a second-order perturbation theory treatment can be applied to the Hamiltonian in eq S1 (Supporting Information) based on the effective Hamiltonian method outlined in ref 41. This results in an effective Frenkel−Holstein Hamiltonian

dx.doi.org/10.1021/jp309407r | J. Phys. Chem. B XXXX, XXX, XXX−XXX

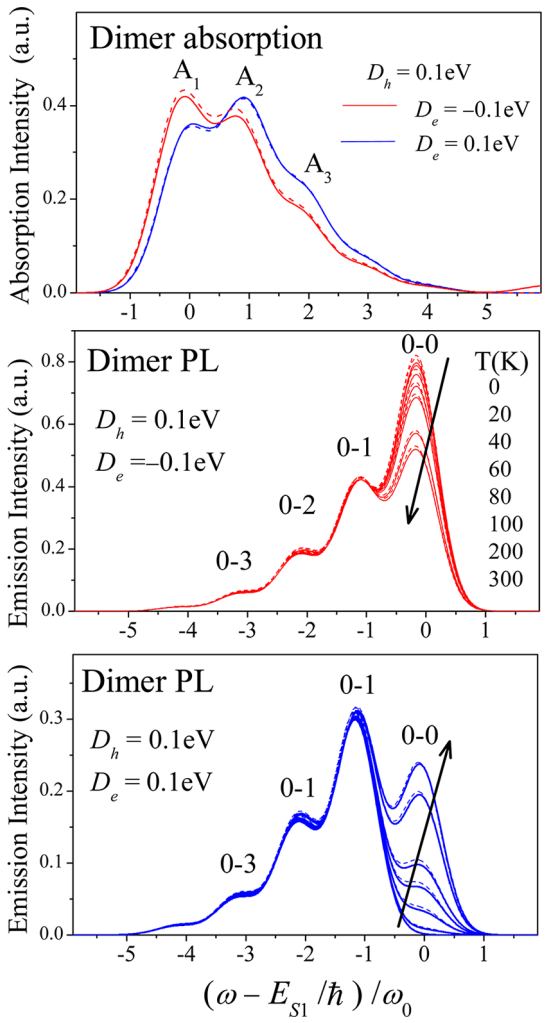

Figure 7. Absorption and (reduced) PL spectra for a WFO coupled C_2 dimer with the indicated values of D_h and D_e. Signs derive from the C_2 phase convention. Red (blue) curves show J-like (H-like) behavior. Solid curves are evaluated using the full Hamiltonian in eq S1 in the Supporting Information. Dashed curves utilize the effective Hamiltonian in eq 12. Arrows in PL spectra indicate increasing temperature. In all cases, $E_{CT} - E_{S_1} = 1.0$ eV, $\hbar\omega_0 = 0.17$ eV, and $\lambda^2 = 1.0$. In the full Hamiltonian, we also took the ionic HR factors to be 0.5.

$$H_F = E_{S_1} + \Delta_{WFO} + \hbar\omega_0 \sum_{n=1,2} b_n^\dagger b_n + \hbar\omega_0 \sum_{n=1,2} \{\lambda(b_n^\dagger + b_n) + \lambda^2\}|n\rangle\langle n| + (J_{WFO} + J_{TS})\{|1\rangle\langle 2| + |2\rangle\langle 1|\} \quad (12)$$

The state $|n\rangle$ indicates that the nth (n = 1, 2) oligomer in the dimer is excited (to the state S_1) while the remaining oligomer is in its ground electron state (S_0). (Hence, $|1\rangle$ and $|2\rangle$ are equivalent to $|A\rangle$ and $|B\rangle$ introduced earlier.) The operators $b_n^\dagger$ and b_n respectively create and annihilate a vibrational quantum of the symmetric stretching mode (with frequency ω_0) on the nth oligomer. The HR factor is λ^2.

The Hamiltonian in eq 12 contains the usual through-space Coulombic coupling, J_{TS}, as well as effective WFO-induced coupling given by

$$J_{WFO} = -\frac{2D_eD_h}{E_{CT} - E_{S_1}} \quad (13a)$$

Interestingly, in the limit defined by eq 11, the two couplings are additive. There is also a diagonal shift in the energies of all eigenstates given by

$$\Delta_{WFO} = -\frac{(D_e^2 + D_h^2)}{E_{CT} - E_{S_1}} \quad (13b)$$

which is intrinsically negative independent of the signs of D_e and D_h.

The dependence of J_{WFO} on the product D_eD_h is consistent with a "two-step" energy transfer, where moving a Frenkel excitation from one oligomer to the other requires the transfer of an electron and then a hole (and vice versa).[19] The term D_e^2 (D_h^2) in Δ_{WFO} in eq 13b arises from an electron (hole) transfer from oligomer A to B, for example, followed by back-transfer to A. In a linear aggregate with periodic boundary conditions, the presence of twice as many nearest neighbors (compared with a dimer) leads to an extra factor on the right-hand side of eq 13b (but not eq 13a).

Note that J_{WFO} in eq 13a is negative when $D_eD_h > 0$. Under the T phase convention, where the bright exciton is symmetric, a negative sign for J_{WFO} places the bright exciton *lower* in energy than the dark exciton, as in a J-aggregate. In an eclipsed dimer which has translational symmetry and an inversion center, one can alternatively use the *i* phase convention where J-aggregation now requires $D_eD_h < 0$ (see eq 7). In this case, J_{WFO} in eq 13a becomes *positive*. However, the bright exciton is now antisymmetric (see eq 2), so that a positive sign for J_{WFO} also places the bright exciton *lower* in energy than the dark exciton, as in a J-aggregate. Hence, the photophysical properties remain independent of the chosen phase convention.

In ref 35, a very similar Hamiltonian to eq 12 was derived (see eq 25 in that work) but for a *single* P3HT chain, viewed as a linear aggregate of head-to-tail coupled thiophene units. Hence, J_{WFO} in eq 13a was more appropriately labeled as J_{intra} to indicate *intra*chain through-bond coupling between adjacent rings as mediated by the electron (t_e) and hole (t_h) transfer integrals. Under the T-phase convention, t_e and t_h were taken to be equal (equivalent to $D_e = D_h$ here), making J_{intra} negative and bestowing J-aggregate photophysics onto the chain. Such behavior has been demonstrated in single polydiacetylene chains by Schott and co-workers.[42−44] The second-order downward shift of the energies of all states in the polymer chain is $\Delta_{intra} = 2J_{intra}$, equivalent to $\Delta_{WFO} = 2J_{WFO}$ obtained from eqs 13a and 13b after setting $D_e = D_h$ and accounting for a doubling of the nearest neighbors in eq 13b. (Note that a typo in eq 25 of ref 35 resulted in a negative sign in front of $2J_{intra}$.)

An important check on the Hamiltonian in eq 12 is provided in the limit where vibronic coupling and through-space coupling are absent. In this limit, the dimer energies are simply

$$E_\pm = E_{S_1} + \Delta_{WFO} \pm J_{WFO} \quad (14)$$

After inserting Δ_{WFO} and J_{WFO} from eqs 13a and 13b into eq 14, we obtain

$$E_\pm = E_{S_1} - \frac{(D_e \pm D_h)^2}{E_{CT} - E_{S_1}} \quad (15)$$

which agrees exactly with the level energies predicted using second-order perturbation theory in eqs 9a and 9b.

dx.doi.org/10.1021/jp309407r | J. Phys. Chem. B XXXX, XXX, XXX−XXX

The dashed curves in Figure 7 show the spectral calculations using the effective Hamiltonian. The agreement with the spectra based on the full Hamiltonian in eq S1 (Supporting Information) is very good, since the condition in eq 11 is maintained.

V. APPLICATIONS TO P3HT

In the remainder of this work, we focus on WFO coupling in P3HT π-stacks, where $E_{CT} - E_{S_1} \approx 0.5$ eV, as estimated by Deibel et al. using photoemission spectroscopy.[45] Here, the CT state corresponds to the polaron pair. In order to evaluate the coupling between neighboring molecules, we consider the C_i dimer and adapt the translation phase convention; see eq 10. Inserting 0.5 eV into the denominator of eq 13a along with the values of D_e and D_h extracted from the 8T calculations in Figure 4b gives the WFO couplings (J_{WFO}) in the contour plot in Figure 8. (Note that in order to adhere to the T-phase convention the sign of the product D_eD_h is changed relative to that obtained under the i convention of eq 7.) Positive (negative) values for J_{WFO} indicate H- (J-) aggregation, as indicated by the blue (red) regions in Figure 8.

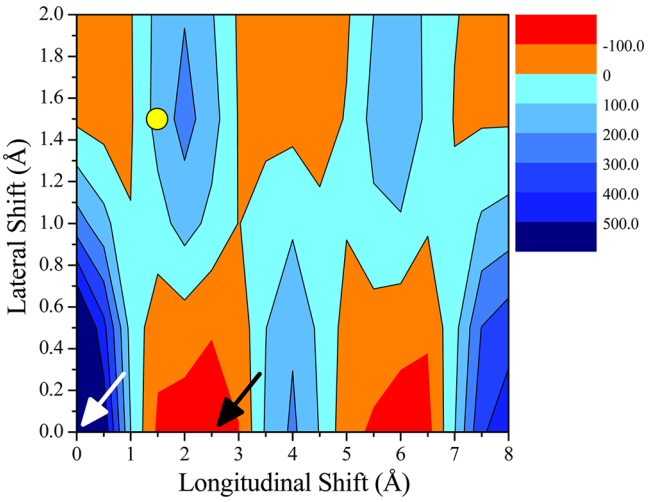

Figure 8. Calculated values for J_{WFO} (in cm^{-1}) between two 8T's in a C_i dimer as a function of longitudinal and lateral displacements. Molecular planes are separated by 3.8 Å. Blue (red) regions correspond to H- (J-) aggregates. Maximum and minimum couplings are indicated by the arrows. The origin corresponds to the eclipsed dimer in Figure 2b. (See text for details.)

The figure shows that the maximum value, $J_{WFO} = 907$ cm^{-1}, occurs when neighboring chains are eclipsed (see Figure 2b), corresponding to the point (0,0) in Figure 8. Such π-stacks will behave as strongly coupled H-aggregates. The minimum coupling, $J_{WFO} = -180$ cm^{-1}, occurs when the neighboring chains are shifted by approximately 2.5 Å along the long molecular axis but with no lateral shift. With this geometry, J-aggregate behavior is expected. In making J/H assignments, it is assumed that Coulombic coupling is negligible, as would exist in long polymer chains.

The spectra corresponding to 8T dimers configured at the extreme points are shown in Figure 9. The vibronic signatures are once again consistent with our assignment of H- and J-aggregation based on the sign of D_eD_h. The agreement between the spectra evaluated using the effective and full Hamiltonians is still quite good, despite the reduced Frenkel/CT splitting used in Figure 9, making the inequality in eq 11 more difficult to justify.

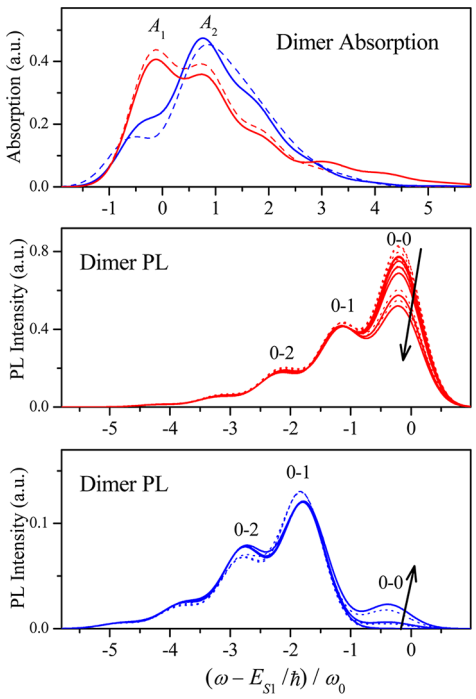

Figure 9. Absorption and (reduced) PL spectra for 8T (C_i) dimers. Blue curves correspond to H-dimers represented by the point (0,0) in Figure 8 ($D_e = -1231$ cm^{-1} and $D_h = 1485$ cm^{-1} under the T sign convention). Red curves correspond to J-dimers represented by the point (2.5,0) in Figure 8 ($D_e = 422$ cm^{-1} and $D_h = 861$ cm^{-1}). Solid curves are obtained using the full Hamiltonian in eq S1 (Supporting Information), while dashed curves utilize the effective Hamiltonian in eq 12. Arrows in PL spectra indicate increasing temperature, for the T values of Figure 7. In all cases, $E_{CT} - E_{S_1} = 0.5$ eV, $J_{TS} = 0$, $\hbar\omega_0 = 0.17$ eV, and $\lambda^2 = 1.0$. In the full Hamiltonian, we also took the ionic HR factors to be 0.5.

In the most common polymorph of P3HT (Form I), Brinkmann and co-workers evaluated the longitudinal and lateral displacements to be approximately 1.5 Å each,[46] as indicated by the yellow circle in Figure 8. The phase plot predicts weak H-aggregation with $J_{WFO} \approx 140$ cm^{-1}, significantly less than the value of ~250 cm^{-1} obtained for P3HT films spin-cast from chloroform[47] based on a measured A_1/A_2 intensity ratio of about 0.65. Figure 10 shows the calculated absorption spectrum for a WFO coupled 10mer. The A_1/A_2 intensity ratio (≈0.80) is larger than the measured ratio. Increased coupling *lowers* the ratio in H-aggregates, suggesting that additional interchain Coulombic coupling is needed to account for the experimental spectrum.

VI. CONCLUSION

We have shown herein that J- and H-aggregates can be created by the WFO coupling induced by Frenkel/CT exciton mixing in cases where the conventional Coulombic coupling is much smaller by comparison. For a linear aggregate with one molecule per unit cell, WFO coupling involving primarily the HOMO and LUMO levels on each chromophore places the bright exciton on the top of the band, as in an H-aggregate, when the product of the electron and hole dissociation integrals, D_eD_h, is negative. Conversely, the bright exciton resides at the band bottom, as in a J-aggregate, when $D_eD_h > 0$.

dx.doi.org/10.1021/jp309407r | J. Phys. Chem. B XXXX, XXX, XXX–XXX

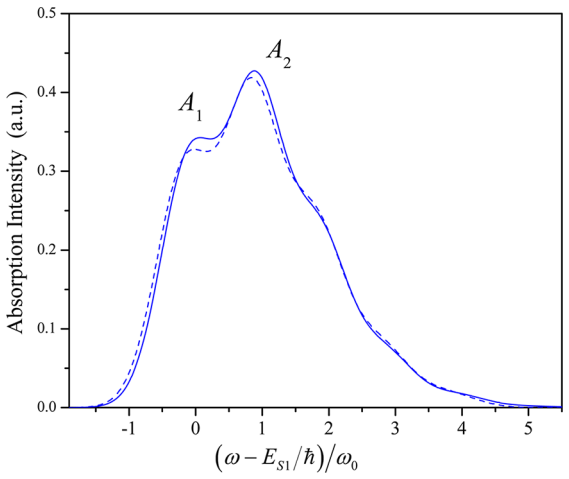

Figure 10. Absorption spectrum for a π-stack containing 10 8T chromophores. Coulombic coupling is not included. Solid curves are obtained using the full Hamiltonian in eq S1 (Supporting Information), while dashed curves utilize the effective Hamiltonian in eq 12. (Both Hamiltonians are modified for >2 chromophores.) D_e and D_h are evaluated for a relative orientation (1.5,1.5) between neighboring chromophores. In addition, $E_{CT} - E_{S_1} = 0.5$ eV, $\hbar\omega_0 = 0.17$ eV, and $\lambda^2 = 1.0$. In the full Hamiltonian, we also took the ionic HR factors to be 0.5.

(Here, the signs of D_e and D_h are based on the translation operation convention; see the discussion preceding eq 10.) Moreover, WFO coupled H-aggregates are indirect bandgap semiconductors, while J-aggregates are direct bandgap semiconductors. The vibronic spectral signatures of J- and H-aggregates derived from WFO coupling are essentially identical to those displayed by their Coulomb coupled counterparts. A second-order perturbative treatment of the Frenkel/CT Hamiltonian results in an effective Frenkel Hamiltonian (eq 12), which clearly identifies the forms of the WFO coupling and energy shift in eqs 13a and 13b, respectively.

There is, however, one property which distinguishes WFO coupled J/H-aggregates from their Coulomb coupled counterparts. As shown in Figure 9, the absorption spectra of both (WFO coupled) aggregate types are *red-shifted* relative to the monomer. This contrasts the well-known behavior displayed by Coulomb coupled aggregates: J-aggregates are red-shifted, *but* H-aggregates are blue-shifted. The universal red-shift in WFO coupled dimers arises from the repulsion of *both* bright and dark excitons to lower energies through interaction with the higher-energy CT states, as can be appreciated from eqs 9a and 9b in the case of no vibronic coupling. A special case occurs when $D_e = D_h$ under the C_2 convention (or $D_e = -D_h$ under the T convention). In this case, the bright exciton is not shifted, since the coupling to the same-symmetry CT state is exactly zero (see Figure 6b), while the dark state shifts to lower energies, creating an H-aggregate. However, when vibronic coupling is included, both bright and dark states are shifted downward in energy, causing a pronounced red-shift in the absorption spectrum relative to the monomer (see Figure 9).

In this work, we have assumed that the intermolecular electron and hole transfer integrals are independent of nuclear degrees of freedom, which may not always be a valid approximation.[48] In particular, lattice phonons, which serve to modulate the intermolecular distance, may lead to changes in t_{HOMO} and t_{LUMO}. The resulting coupling between the nuclear and electronic degrees of freedom can lead to excimer formation which has been observed in perylene diimide sandwich complexes,[49] for example, but not in the P3HT π-stacks studied here. The PL from P3HT films has a well-defined vibronic structure[47,50] and does not display a strongly red-shifted and unstructured PL line shape typical of excimers.

We have shown in a previous work[16] that Frenkel/CT exciton mixing leads to an effective (WFO) coupling between the two inequivalent lattices in crystalline tetracene. The WFO coupling dominates through-space Coulombic coupling near the absorption origin, making CT largely responsible for the resulting Davydov splitting.[16] The polarized absorption spectrum normal to the ac-plane displays a dominant 0−0 peak, with the 0−0/0−1 ratio 2−3 times larger than what is found in monomeric tetracene, a clear signature of J-aggregation. The latter arises almost entirely from WFO coupling, since it persists even when the Coulombic coupling is set to zero. Interestingly, the higher-energy Davydov component is polarized along the *a*-axis and is H-like. In this example, the weak Coulombic coupling is mainly due to the small oscillator strength associated with $S_0 \rightarrow S_1$ transition, polarized mainly along the short molecular axis of tetracene.

In polymer aggregates, Coulombic coupling between adjacent chains leads to classic H-aggregate behavior, with the magnitude of the excitonic coupling practically vanishing as the chain length, L, increases.[9,23−26] For cofacial nT oligomers separated by 4 Å, the Coulombic coupling decreases from roughly 1000 cm^{-1} for terthiophene ($n = 3$) to less than 100 cm^{-1} for $n > 40$ rings.[26] Conversely, the charge transfer integrals t_{HOMO} and t_{LUMO} responsible for WFO coupling are only weakly dependent on the oligomer length.[26] Taking $|J_{WFO}| \approx 100$ cm^{-1} from the analysis in section V results in dominant WFO coupling in polymer aggregates with conjugation lengths exceeding approximately 40 rings.

We have recently shown that *single* P3HT chains possess the properties of linear J-aggregates, where the latter can be understood as though-bond coupled "head-to-tail" thiophene units.[38] Assuming a positive (H-like) coupling between two such chains leads to interesting hybrid H/J properties due to the competition between intrachain (J-favoring) and interchain (H-favoring) interactions.[35] The predictions based on the HJ-aggregate model in ref 35 are independent of the source of the interchain coupling, be it Coulombic or WFO, as long as it is positive (H-like). Recently, P3HT nanofibers have been shown to display J-aggregate vibronic signatures, in particular, absorption and PL spectra with dominant 0−0 peaks,[29] in stark contrast to the H-aggregate behavior observed in spin-cast films, where such peaks are far less intense.[47,50] In refs 29 and 35, it was shown that the nanofiber photophysics likely result from the aforementioned dominance of intrachain interactions brought about by superior intrachain order. The current work admits the interesting possibility of polymer "JJ-aggregates" in which intrachain *and* interchain couplings are negative. The photophysical properties of such aggregates would differ substantially from the predictions of the HJ-aggregate model.[35] For example, whereas superradiance requires thermal activation in HJ-aggregates, no such activation would be required in JJ-aggregates, which would therefore display much higher radiative decay rates. Such aggregates could possibly be used to make more efficient light emitting diodes.

In polymer π-stacks, the sign of the WFO coupling depends mainly on the longitudinal shift between neighboring chains due to the mixing of the interchain polaron and the intrachain Frenkel exciton. Figure 8 shows that a longitudinal shift of

approximately 1.5 Å, coincident with a lateral shift of less than 0.5 Å, results in a JJ-aggregate in P3HT. Polymorphism in poly(3-alkylthiophenes) (P3ATs) was established early on by Prosa.[36,37] Thus far, two forms of P3ATs are known. For P3HT, Form I is the thermodynamically stable form and is characterized by longitudinal and lateral shifts of approximately 1.5 Å (yellow circle in Figure 8).[46] In Form II—readily observed in poly(3-butylthiophene)—the two chains appear to be close to the staggered configuration shown in Figure 2a. Figure 8 shows that the longitudinal and lateral shifts expected for both Forms I and II are consistent with WFO coupled H-aggregate behavior. To enforce the longitudinally displaced orientation favorable for J-aggregates may require chemical tuning of the side groups. We are currently investigating in greater detail the implications of the JJ-aggregate model.

■ ASSOCIATED CONTENT

Supporting Information

Details concerning the Frenkel-CT Hamiltonian and the evaluation of spectral observables. This material is available free of charge via the Internet at http://pubs.acs.org.

■ AUTHOR INFORMATION

Notes

The authors declare no competing financial interest.

■ ACKNOWLEDGMENTS

F.C.S. is supported by the National Science Foundation, Grant No. DMR-1203811.

■ REFERENCES

(1) Kasha, M. *Radiat. Res.* **1963**, *20*, 55−70.
(2) Spano, F. C. *Acc. Chem. Res.* **2010**, *43*, 429−439.
(3) Spano, F. C. *J. Am. Chem. Soc.* **2009**, *131*, 4267−4278.
(4) Forster, T. *Ann. Phys.* **1948**, *437*, 55.
(5) Scholes, G. D. *Annu. Rev. Phys. Chem.* **2003**, *54*, 57−87.
(6) Scholes, G. D.; Fleming, G. R. *J. Phys. Chem. B* **2000**, *104*, 1854−1868.
(7) Pullerits, T.; Chachisvilis, M.; Sundstrom, V. *J. Phys. Chem.* **1996**, *100*, 10787−10792.
(8) Wong, K. F.; Bagchi, B.; Rossky, P. J. *J. Phys. Chem. A* **2004**, *108*, 5752−5763.
(9) Barford, W. *J. Chem. Phys.* **2007**, *126*, 134905.
(10) Megow, J.; Roder, B.; Kulesza, A.; Bonacic-Koutecky, V.; May, V. *ChemPhysChem* **2011**, *12*, 645−656.
(11) Jang, S. J.; Newton, M. D.; Silbey, R. J. *Phys. Rev. Lett.* **2004**, *92*, 218301.
(12) Tretiak, S.; Middleton, C.; Chernyak, V.; Mukamel, S. *J. Phys. Chem. B* **2000**, *104*, 9540−9553.
(13) Sebastian, L.; Weiser, G.; Bässler, H. *Chem. Phys.* **1981**, *61*, 125−135.
(14) Sebastian, L.; Weiser, G.; Peter, G.; Bässler, H. *Chem. Phys.* **1983**, *75*, 103−114.
(15) Zhu, X. Y.; Yang, Q.; Muntwiler, M. *Acc. Chem. Res.* **2009**, *42*, 1779−1787.
(16) Yamagata, H.; Norton, J.; Hontz, E.; Olivier, Y.; Beljonne, D.; Bredas, J. L.; Silbey, R. J.; Spano, F. C. *J. Chem. Phys.* **2011**, *134*, 204703.
(17) Stradomska, A.; Kulig, W.; Slawik, M.; Petelenz, P. *J. Chem. Phys.* **2011**, *134*, 224505.
(18) Harcourt, R. D.; Scholes, G. D.; Ghiggino, K. P. *J. Chem. Phys.* **1994**, *101*, 10521−10525.
(19) Harcourt, R. D.; Ghiggino, K. P.; Scholes, G. D.; Speiser, S. *J. Chem. Phys.* **1996**, *105*, 1897−1901.
(20) Dexter, D. L. *J. Chem. Phys.* **1953**, *21*, 836.
(21) Yan, M.; Rothberg, L. J.; Kwock, E. W.; Miller, T. M. *Phys. Rev. Lett.* **1995**, *75*, 1992−1995.
(22) Jiang, X. M.; Õsterbacka, R.; Korovyanko, O.; An, C. P.; Horovitz, B.; Janssen, R. A. J.; Vardeny, Z. V. *Adv. Funct. Mater.* **2002**, *12*, 587−597.
(23) Soos, Z. G.; Hayden, G. W.; McWilliams, P. C. M.; Etemad, S. *J. Chem. Phys.* **1990**, *93*, 7439−7448.
(24) Manas, E. S.; Spano, F. C. *J. Chem. Phys.* **1998**, *109*, 8087.
(25) Cornil, J.; dos Santos, D. A.; Crispin, X.; Silbey, R.; Bredas, J. L. *J. Am. Chem. Soc.* **1998**, *120*, 1289.
(26) Gierschner, J.; Huang, Y. S.; Van Averbeke, B.; Cornil, J.; Friend, R. H.; Beljonne, D. *J. Chem. Phys.* **2009**, *130*, 044105.
(27) Psiachos, D.; Mazumdar, S. *Phys. Rev. B* **2009**, *79*, 155106.
(28) Aryanpour, K.; Sheng, C. X.; Olejnik, E.; Pandit, B.; Psiachos, D.; Mazumdar, S.; Vardeny, Z. V. *Phys. Rev. B* **2011**, *83*, 155124.
(29) Niles, E. T.; Roehling, J. D.; Yamagata, H.; Wise, A. J.; Spano, F. C.; Moule, A. J.; Grey, J. K. *J. Phys. Chem. Lett.* **2012**, *3*, 259−263.
(30) Bredas, J. L.; Calbert, J. P.; da Silva, D. A.; Cornil, J. *Proc. Natl. Acad. Sci. U.S.A.* **2002**, *99*, 5804−5809.
(31) Bredas, J. L.; Beljonne, D.; Coropceanu, V.; Cornil, J. *Chem. Rev.* **2004**, *104*, 4971−5003.
(32) Coropceanu, V.; Cornil, J.; da Silva, D. A.; Olivier, Y.; Silbey, R.; Bredas, J. L. *Chem. Rev.* **2007**, *107*, 926−952.
(33) Niedzialek, D.; Lemaur, V.; Dudenko, D.; Shu, J.; Hansen, M. R.; Andreasen, J. W.; Pisula, W.; Müllen, K.; Cornil, J.; Beljonne, D. *Adv. Mater.* [Online early access]. DOI: 10.1002/adma.201201058. Published Online: June 19, **2012**.
(34) Baghgar, M.; Labastide, J.; Bokel, F.; Dujovne, I.; McKenna, A.; Barnes, A. M.; Pentzer, E.; Emrick, T.; Hayward, R.; Barnes, M. D. *J. Phys. Chem. Lett.* **2012**, *3*, 1674−1679.
(35) Yamagata, H.; Spano, F. C. *J. Chem. Phys.* **2012**, *136*, 184901.
(36) Prosa, T. J.; Winokur, M. J.; McCullough, R. D. *Macromolecules* **1996**, *29*, 3654−3656.
(37) Prosa, T. J.; Winokur, M. J.; Moulton, J.; Smith, P.; Heeger, A. J. *Macromolecules* **1992**, *25*, 4364−4372.
(38) Yamagata, H.; Spano, F. C. *J. Chem. Phys.* **2011**, *135*, 054906.
(39) Merrifield, R. E. *J. Chem. Phys.* **1961**, *34*, 1835−1839.
(40) Holstein, T. *Ann. Phys.* **1959**, *8*, 325−342.
(41) Cohen-Tannoudji, C.; Dupont-Roc, J.; Grynberg, G. *Atom-Photon Interactions*; Wiley-Interscience: New York, 1988.
(42) Dubin, F.; Berrehar, J.; Grousson, R.; Schott, M.; Voliotis, V. *Phys Rev. B* **2006**, *73*, 121302.
(43) Lecuiller, R.; Berrehar, J.; Ganiere, J. D.; Lapersonne-Meyer, C.; Lavallard, P.; Schott, M. *Phys Rev. B* **2002**, *66*, 125205.
(44) Schott, M. Optical properties of single conjugated polymer chains (Polydiacetylenes). In *Photophysics of molecular materials: from single molecules to single crystals*; Lanzani, G., Ed.; Wiley-VCH: Weinheim, Germany, 2006; pp 49−145.
(45) Deibel, C.; Mack, D.; Gorenflot, J.; Scholl, A.; Krause, S.; Reinert, F.; Rauh, D.; Dyakonov, V. *Phys. Rev. B* **2010**, *81*, 085202.
(46) Brinkmann, M. *J. Polym. Sci., Part B: Polym. Phys.* **2011**, *49*, 1218−1233.
(47) Clark, J.; Silva, C.; Friend, R. H.; Spano, F. C. *Phys. Rev. Lett.* **2007**, *98*, 206406.
(48) Thompson, A. L.; Gaab, K. M.; Xu, J.; Bardeen, C. J.; Martinez, T. J. *J. Phys. Chem. A* **2004**, *108*, 671−682.
(49) Fink, R. F.; Seibt, J.; Engel, V.; Renz, M.; Kaupp, M.; Lochbrunner, S.; Zhao, H. M.; Pfister, J.; Wurthner, F.; Engels, B. *J. Am. Chem. Soc.* **2008**, *130*, 12858−12859.
(50) Brown, P. J.; Thomas, S. D.; Kohler, A.; Wilson, J. S.; Kim, J.-S.; Ramsdale, C. M.; Sirringhaus, H.; Friend, R. H. *Phys. Rev. B* **2003**, *67*, 064203.